Observability and UV coverage

Damien Ségransan

Observatoire de Genève, 51 chemin des Maillettes, CH-1290, Sauverny, Switzerland

1 Introduction

Baselines selection and/or array configuration is a crucial step when observing with a stellar interferometer. The efficiency and the quality of the observation strongly depend on this step. Furthemore, since images will not be obtained on a regular basis in the next few years with the VLTI due to the limited number of telescopes, observers will depend on model fitting. A good knowledge of the scientific target is thus required to select the points on the uv-plane which will better constrain the model. To do so, as much knowledge as possible about the scientific target is required (angular size, orientation, survey, single-shot observation) as well as a good understanding of the interferometer characteristics like the available number of telescopes and stations, the delay lines stroke and possible dome vignetting. Observers thus need "tools", like ASPRO to efficiently prepare the observations.

The first part of this tutorial is a reminder of the uv-plane coverage with a stellar interferometer and of the possible limitation due to the delay lines. The second part is a short demonstration of the software ASPRO, which will help you do the Practice Work Session number 2 (hereafter, PWS2).

2 UV-coverage and delay-line stroke

2.1 UV-plane

Spatial frequencies, $\vec{f} = (u, v)$, are the conjugated coordinates of the spatial coordinates (x, y) in the image plane. While (x, y) measure angles, usually expressed in *arcseconds*, spatial frequencies measure distances in the incident wavefront measured in wavelength units (equation 1). They are usually expressed in $arcseconds^{-1}$.

$$\vec{f} = (u, v) = \frac{1}{\lambda} (\Delta X, \Delta Y) \tag{1}$$

During the imaging process (this volume, C. Hanniff lecture), a single dish telescope can be viewed as a low pass filter with cut-off frequency D/λ where D is the telescope diameter and λ is the wavelength. The incoming wavefront is thus spatially filtered by the telescope and all spatial frequencies up to the cut-off frequency are transmitted. The point spread function is simply the impulse response of the filter.

Figure 1 illustrates the imaging process viewed as a filtering process of the incoming wavefront. The image on figure 1*a* represents a binary star observed at the Canada-France-Hawaii Telescope with the Adaptive Optics Bonnette PUE'O (*Cf.* [**?**]) in the K band (2.2 μm). The Airy rings are clearly seen and the diffraction limit of this 3.6-meter-telescope is easely reached in K ($\lambda/D = 0.126$ arcsec). The Fourier components (visibility) of the binary star are represented on figure 1*b*. In this peculiar case, the visibility is a sinusoid which period is related to the angular separation of the binary, its orientation to the position angle and the amplitude to the flux ratio (see appendix in PWS2). All spatial frequencies are transmitted up to the cut-off frequency of the telescope, which is $D/\lambda = 7.93$ arcsec^{-1} in K. This corresponds

to the inverse of the classical diffraction limit of the telescope.

Fig. 1. Resolved binary star observed at $2.2\mu m$ at the Canada-France-Hawaii Telescope with adaptive optics. The left-hand side figure shows the image of the binary star while the right-hand side figure shows the Fourier components of the binary star. All spatial frequencies are transmitted up to the cut-off frequency of the telescope, which is $D/\lambda = 7.93$ arcsec^{-1}.

When observing with a stellar interferometer, the sampling of the incident wavefront is no longer continuous and depends on the array configuration. The Fourier components of the object are individually measured at different spatial frequencies. This is exactly what the Zernike-Van Citter theorem states :

The complex degree of coherence at zero OPD is equal to the normalized Fourier transform of the object luminosity distribution

The mathematical expression of the theorem is :

$$V\left(\frac{\vec{B}}{\lambda}\right) = V\left(u,v\right) = \frac{\hat{I}\left(u,v\right)}{\hat{I}\left(0,0\right)} \tag{2}$$

where V is the visibility, $\hat{I}$ is the Fourier transform of the object of interest and $\vec{B}$ represents the baseline vector, which is defined as the difference of coordinates between the telescopes.

$$\vec{B} = \Delta X\vec{i} + \Delta Y\vec{j} + \Delta Z\vec{k} \tag{3}$$

where $\vec{i}$, $\vec{j}$ and $\vec{k}$ point respectively toward the East, the North and the Meridian.

We should emphasize that a stellar interferometer measures only one visibility per baseline. The efficiency is thus extremely low compared to direct imaging but some nice tricks allow to improve the observing efficiency.

2.2 Filling the uv-plane

Figure 1b shows that the sinusoid characteristics (that is the binary parameters) could have been recovered with a only a few points in the uv-plane provided that they were well selected. This shows how easy, simple target characterisation is, using stellar interferometry.
In order to do so, we have to understand the constraints on uv-sampling caused by Michelson stellar interferometers (as opposed to Fizeau).
Actually, when discussing the uv-plane coverage, the quantity of interest is not the baseline vector itself but the projected baseline vector on the sky which depends on the source declination and the hour angle. Equation 4 relates the baseline vector to the sampled spatial frequencies of a target of declination δ and hour angle h. It shows the benefit of the earth rotation to cover the uv-plane.

$$\begin{pmatrix} u \\ v \\ w \end{pmatrix} = \frac{1}{\lambda} \begin{pmatrix} \sin(h) & \cos(h) & 0 \\ -\sin(\delta)\cos(h) & \sin(\delta)\sin(h) & \cos(\delta) \\ \cos(\delta)\cos(h) & -\cos(\delta)\sin(h) & \sin(\delta) \end{pmatrix} \begin{pmatrix} \Delta X \\ \Delta Y \\ \Delta Z \end{pmatrix} \quad (4)$$

When eliminating the hour angle from equation 4, we get the so-called *uv-tracks*, (equation 5) which correspond to the spatial frequencies sampling due to the earth rotation when observing a target of declination δ. **uv-tracks are ellipses** (*Cf.* equation 5

and figure 2).

$$u^2 + \left(\frac{v - (\Delta Z/\lambda)\cos(\delta)}{\sin(\delta)} \right)^2 = \frac{\Delta X^2 + \Delta Y^2}{\lambda^2} \tag{5}$$

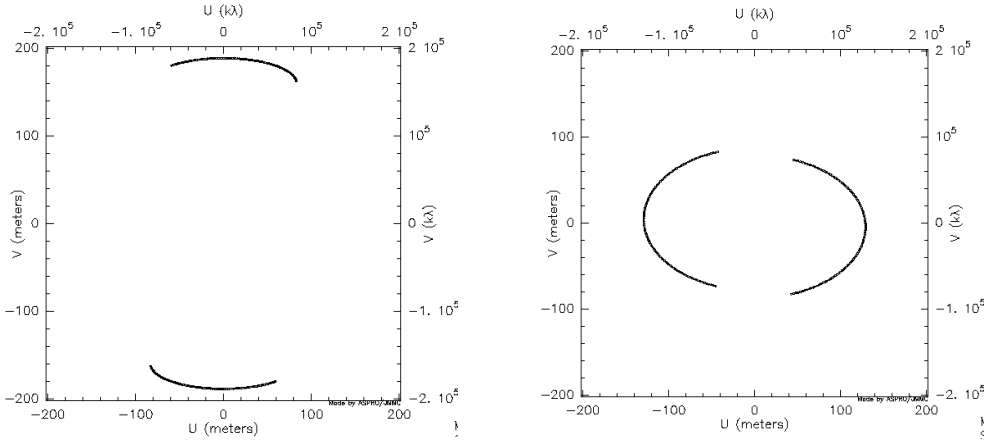

Fig. 2. UV-coverage for a 2-telescope-interferometer and 2 different configurations. The left-hand side figure corresponds to a source of declination -20 degrees and a 200-meter North-South baseline while the right-hand side figure corresponds to a source of declination -40 degrees and a 130-meter-baseline oriented East-West

A second solution to cover the uv-plane (and the more expensive one) is to add telescopes to the array. Figure 2 represents the UV-coverage for a 2-telescope-configuration while figure 3 represents the UV-coverage for a 3-telescope-array. One should notice that observing with three telescopes instead of two represents a major gain in observing efficiency. One simultaneously measure visibilities at three baselines instead of one. The number of baseline as a function of the number of telescope is given in equation 6.

$$N_b = n_t.\,(n_t - 1)\,/2 \tag{6}$$

A third solution to improve the uv-plane sampling is to use spectral resolution. If we assume that the object of interest has the same characteristics over a spectral region, spectral resolution will greatly improve the uv-coverage as shown on figure 4 for a two and a three telescope array simultaneously observing in J, H

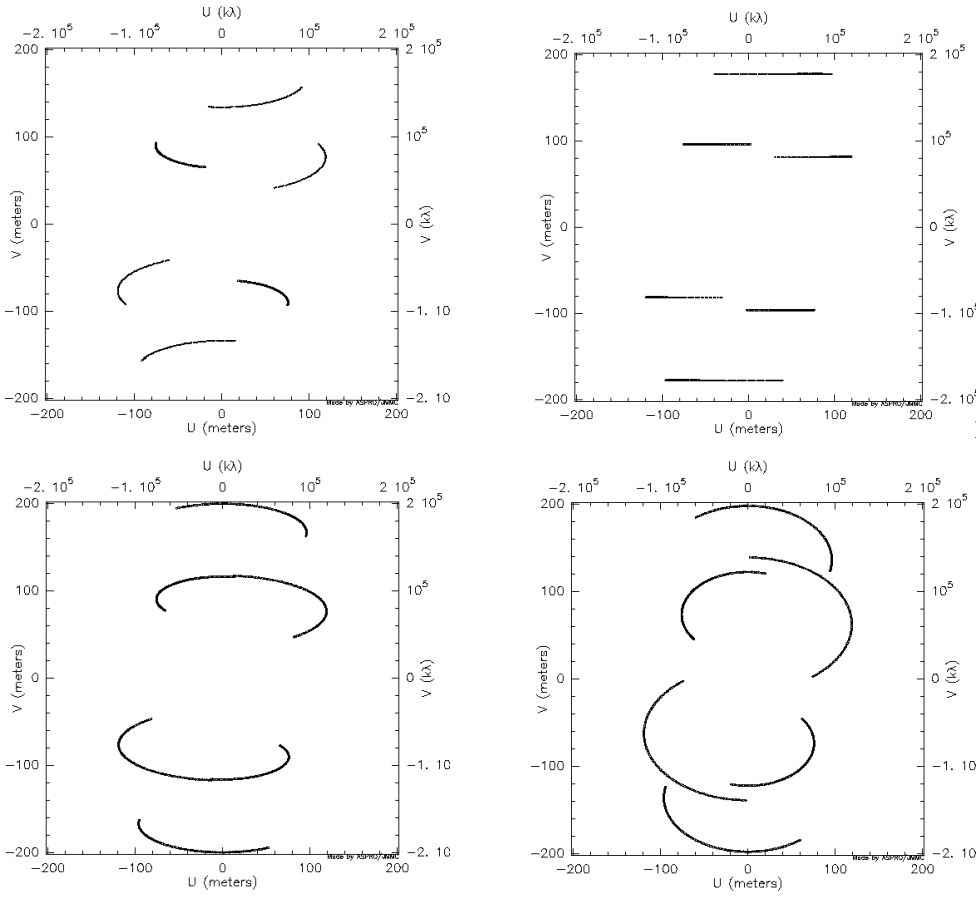

Fig. 3. UV-coverage for a 3-telescope-interferometer. The top left-hand side figure corresponds to a source of declination +20 degree and the top right-hand side figure to a declination of 0.0 degree. The bottom left-hand side figure corresponds to a source of declination -20 degree and the bottom right-hand side figure to a declination of -40 degree.

and K.

What should be remembered to improve the UV-Sampling:

- Use the earth rotation
- Change the array configuration
- Use spectral resolution
- Add telescopes to the array

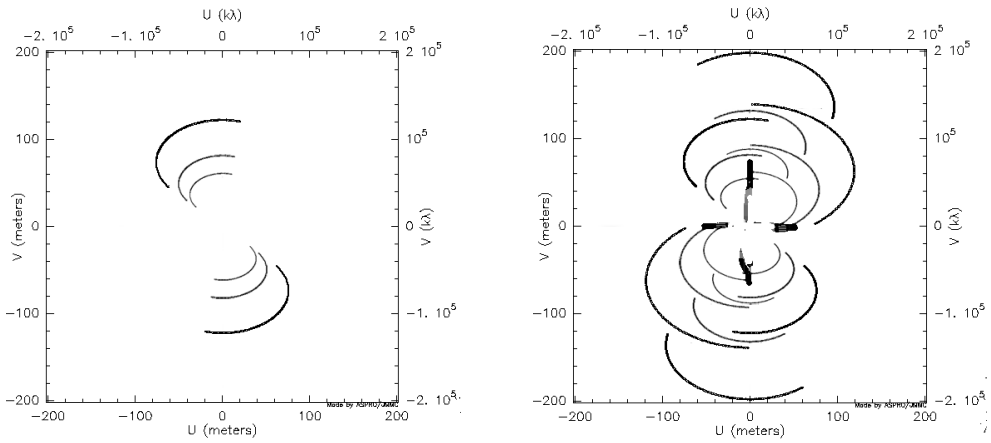

Fig. 4. UV-coverage for a 2 and a 3-telescope-interferometer simultaneously observing in J, H and K.

2.3 Delay-line stroke

So far, we have learned that spatial frequency sampling is not continuous when observing with an interferometer and that the uv-plane is mostly empty! An additional important observing/technical constraint is the delay line stroke. The Optical Path Difference (OPD) that must be compensated when observing with a stellar interferometer is given in equation 7.

$$OPD = w + OPD_{int} = \vec{B}.\vec{s} + OPD_{int} \tag{7}$$

where s is the unit vector pointing into the source direction and is defined in equation 8 and OPD_{int} is the internal OPD of the interferometer.

$$\vec{s} = [\cos(alt)\cos(az), \cos(alt)\sin(az), \sin(alt)] \tag{8}$$

az is the azimuth and alt is the altitude. They are defined in equations 9 and 10

$$\sin(alt) = \sin(\delta)\ \sin(l) + \cos(\delta)\ \cos(l)\ \cos(h) \tag{9}$$

and

$$\tan(az) = \frac{-1.\ \cos(\delta)\ \sin(h)}{\sin(\delta)\ \cos(l) - \cos(\delta)\ \cos(h)\ \sin(l)} \tag{10}$$

where l is the latitude, δ is the source declination and h is the hour angle.

Figure 5 illustrates the OPD constraint for 2 different configurations. The first configuration corresponds to a source of declination $\delta = -20$ degrees and a baseline vector oriented North-South of modulus 200 meters. The OPD ranges from -18 meters to 0 meter for 6 hours of observation.
On the other hand, if you choose a source of declination $\delta = -40$ degrees and a baseline vector oriented East-West of modulus 200 meters, then the OPD ranges from -100 meters to +100 meters.

This demonstrates that long delay line strokes are required to be able to observe targets of various declination for a long time. In the case of the VLTI, the optical path range is 120 meters long which allows to observe target between -60 degrees to +20 degrees for 5 hours.

3 Choosing an array configuration using ASPRO

The previous section gave answers on how to fill the gaps in the uv-plane and insisted on possible limitations due to the delay lines. This section, that should be followed by the PWS2, shows how an optimal baseline can be chosen for a given scientific target using the observation preparation tool, ASPRO. In this section, the simple case of star radius measurement is addressed.

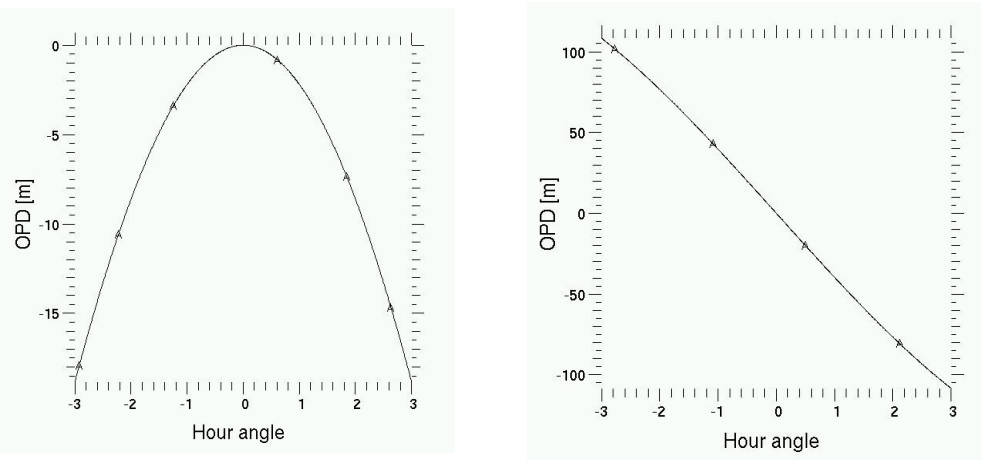

Fig. 5. Optical Path Difference for 2 interferometer configurarions. The left-hand side figure corresponds to a source of declination -20 degrees and a 200-meter baseline vector oriented North-South while the right-hand side figure corresponds to a source of declination -40 degrees and a 200-meter baseline vector oriented East-West

3.1 Radius measurement

Until 2001, only two M dwarfs radii had been directly measured with great accuracy. This was done in the peculiar case of the eclipsing binary YYgem. Direct radius measurements of a few M dwarfs have since been conducted at PTI (Lane et al., 2001) and with the VLTI (Sgransan et al., 2003). The VLTI will be able to directly measure the radii of the closest M dwarfs thanks to its longest baseline ($> 100m$).

Let's consider the M dwarf Gl887, which main characteristics are summarized in table 1.

Table 1
Star main characteristics

Object	Spectral Type	Distance [pc]	J	Ra	Dec	Diameter [mas]
Gl887	M0V	3.3	4.16	23:05:52	-35:51:11	1.37

First, launch ASPRO and the ASPRO main menu will appear (figure 6). It is assumed that you know how to load a catalog and

select an observing date and time (**When**, **Where** and **What** buttons).

Fig. 6. ASPRO main menu

Once this is done, an object model should be used in order to select the optimal baseline configuration. ASPRO has a large choice of functions and we select the lim-darkened disk model.

- Select the **WHAT** button and clik on **Object Model** (figure 7).

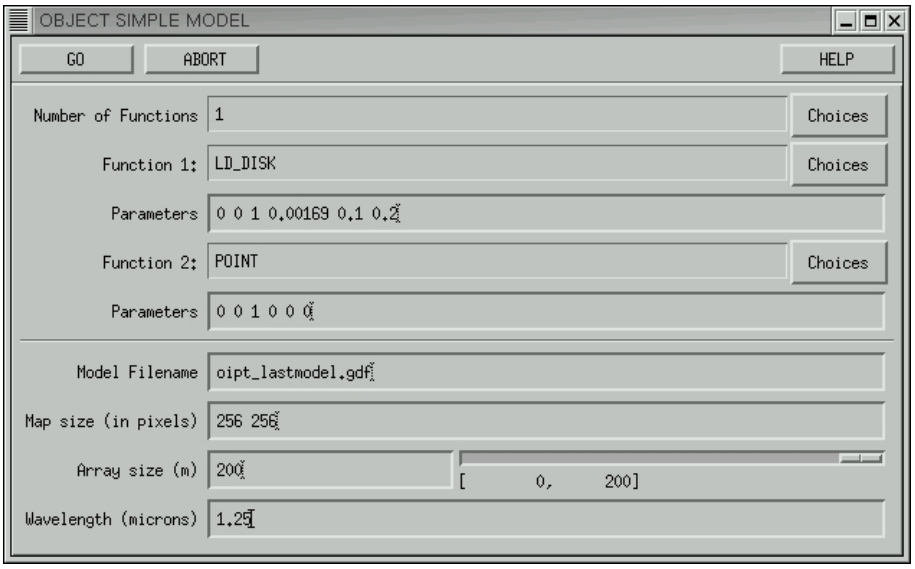

Fig. 7. ASPRO simple modelisation widget.

Once this is done, you need to select a VLT configuration (here a 3-telescope configuration has been selected with telescopes UT1, UT2 and UT3) that will allow to constrain the parameters of your model and check the observability of the source.

- Select **OBSERVABILITY/COVERAGE** and clik on **observability limits due to delay lines**. You can then select a specific object in the catalog and a wavelength (**SELECT OBJECT**) and plot the observability and the delays (**PLOT DELAYS** and figure **??**)

Figure **??** shows that the star can be observed most of the night (top black line) while the other black lines show the period during which the delay lines can compensate the OPD without changing the fixed delay on telescope number (the fixed delay was set to 97.79 meters).

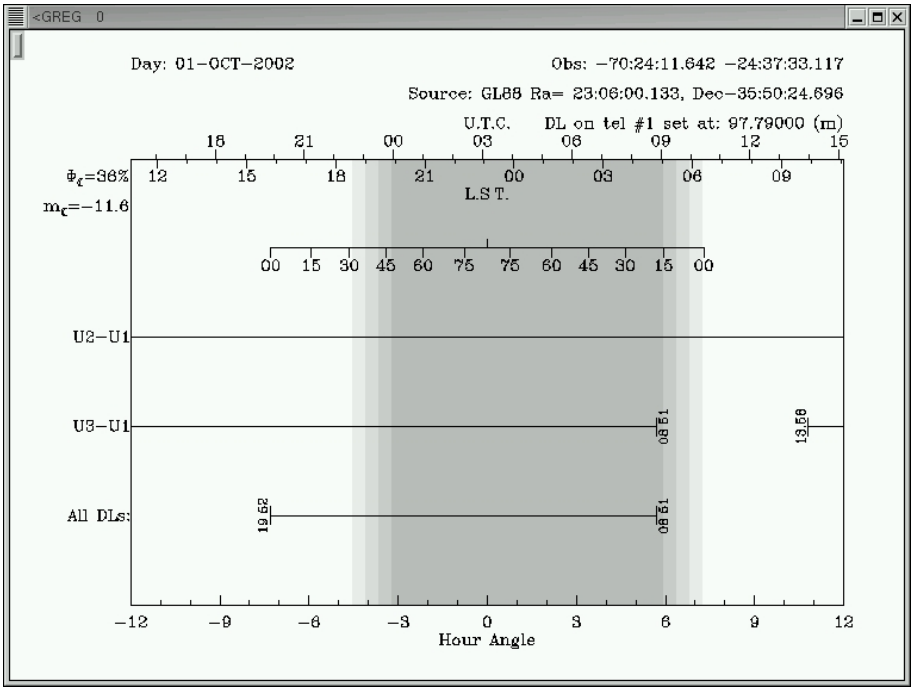

Fig. 8. Observability of Gliese 887

- you can now plot the uv-coverage corresponding to the interferomter configuration (**PLOT UV COVERAGE** and left figure **??**) and check whether the radius is well constrained using this configuration by underplotting the derivative of the visibility with respect to the radius (right figure **??**). Bright regions of the uv-plane show where uv-points constrain the most the radius.

We can see on figure **??** that the chosen array configuration is not optimal to measure the radius of this star.
A good observing strategy to obtain a very accurate radius measurement would be to observe Gl887 with 3 Auxiliary Telescopes and the largest available baselines (the source is bright, there is no need to use the Unitary Telescopes). One could then look for very low visibility amplitude (or very low closure amplitude) or

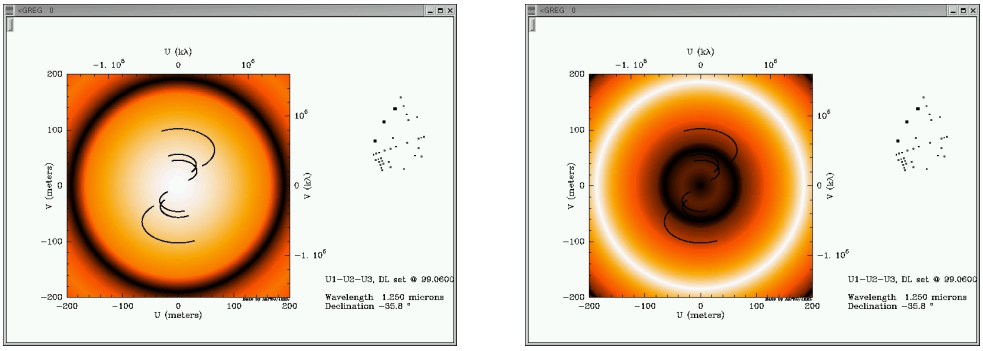

Fig. 9. Visibility model for Gl887 and uv-tracks (left). Derivative of the visibility with respect to the radius. Bright regions show where V(u,v) constrains the most the radius (right)

even better, one could look for 180 degrees shift in the closure phase (*Cf.* J. Young seminar and J. Monnier Tutorial on closure phase).

4 Conclusion

Let's do the Practice Work Session number 2.

References

[1994] Arsenault, R. et al. 1994, SPIES proceedings 2201, Adaptive Optics in Astronomy, p. 833

[2002] Haniff, C., Introduction to interferometry, this school

[2001] Lane, B.F. et al. ApJ 560, 390L, 2001

[2001] Ségransan, D. et al. A&A, 397L, 5, 2003

[2002] Monnier, J., Astrophysics with closure phase, this School

[2002] Ségransan D., Practice Work Session 2, Source observability and UV coverage, this school

[2002] Young, J., From visibilities to science with simple models, this school